Published in final edited form as:
Appl Magn Reson. 2010 December 1; 39(4): 437–451. doi:10.1007/s00723-010-0179-z.

EPR and Quantum Chemical Studies of the pH-sensitive Imidazoline and Imidazolidine Nitroxides with Bulky Substituents

A. A. Bobko,
Institute of Chemical Kinetics and Combustion, Russian Academy of Sciences, Novosibirsk 630090, Russia

Dorothy M. Davis Heart and Lung Research Institute, The Ohio State University, Columbus, OH 43210, USA

I. A. Kirilyuk,
Novosibirsk Institute of Organic Chemistry, Russian Academy of Sciences, Novosibirsk 630090, Russia

N. P. Gritsan,
Institute of Chemical Kinetics and Combustion, Russian Academy of Sciences, Novosibirsk 630090, Russia

D. N. Polovyanenko,
International Tomography Center, Russian Academy of Sciences, Institutskaya 3A, Novosibirsk 630090, Russia

I. A. Grigor'ev,
Novosibirsk Institute of Organic Chemistry, Russian Academy of Sciences, Novosibirsk 630090, Russia

V. V. Khramtsov, and
Dorothy M. Davis Heart and Lung Research Institute, The Ohio State University, Columbus, OH 43210, USA

E. G. Bagryanskaya
International Tomography Center, Russian Academy of Sciences, Institutskaya 3A, Novosibirsk 630090, Russia

E. G. Bagryanskaya: Elena@tomo.nsc.ru

Abstract

The X- and W-band electron paramagnetic resonance (EPR) spectroscopies were employed to investigate a series of imidazolidine nitroxide radicals with different number of ethyl and methyl substituents at positions 2 and 5 of a heterocycle in liquid and frozen solutions. The influence of the substituents on the line shape and width was studied experimentally and analyzed using quantum chemical calculations. Each pair of the geminal ethyl groups in the positions 2 or 5 of the imidazolidine ring was found to produce an additional hyperfine splitting (hfs) of about 0.2 mT in the EPR spectra of the nitroxides. The effect was attributed to the hfs constant of only one of four methylene hydrogen atoms of two geminal ethyl substituents not fully averaged by ethyl group rotation and ring puckering. In accordance with this assumption, the substitution of hydrogen

Correspondence to: E. G. Bagryanskaya, Elena@tomo.nsc.ru.

atoms of CH_2 groups in 2,2,5,5-tetraethyl-substituted imidazolidine nitroxides by deuterium leads to the substantial narrowing of EPR lines which could be useful for many biochemical and biomedical applications, including pH-monitoring. W-band EPR spectra of 2,2,5,5-tetraethyl-substituted imidazolidine nitroxide and its 2,2,5,5-tetraethyl–d_8 deuterium-substituted analog measured at low temperatures demonstrated high sensitivity of their *g*-factors to pH, which indicates their applicability as spin labels possessing high stability.

1 Introduction

Stable nitroxide radicals are used intensively as probes for measurement of oxygen [1, 2], pH [3–5], glutathione [6, 7], redox state [8, 9] in living tissues, for structural studies of biological macromolecules [10], as magnetic resonance imaging contrast agents [11, 12] and in other fields [13–16]. The nitroxide radicals of imidazoline and imidazolidine types were shown to reveal the changes in their electron paramagnetic resonance (EPR) spectra due to reversible protonation of N-3 nitrogen [17] of the radical heterocycle and are widely used as pH-probes [4, 5, 14, 15]. However, instability of the paramagnetic N–O· fragment towards chemical reduction is an unavoidable factor that significantly limits their application, particularly in biological systems. Dependence of nitroxides stability towards reduction on their structure has been the subject of numerous investigations [18–22]. It has been found recently that bulky alkyl groups adjacent to the N–O· fragment significantly increase the stability of nitroxides towards reduction by ascorbate, blood and tissue homogenates [23–26], e.g., 3,4-dimethyl-2,2,5,5-tetraethylimidazolidine-1-oxyl (In4, see Scheme 1) showed 40 times lower rate of reduction by ascorbate than its 2,2,5,5-tetramethyl analogue (In1, Scheme 1). These radicals have pH-dependent EPR spectra with pK_a in the physiological range of pH from 4 to 6, and their enhanced stability towards reduction is very important for in vivo and in vitro pH assessment in biological systems. However, introduction of several bulky alkyl groups to α-carbons of nitroxide moiety may lead to significant broadening of EPR lines, which demolishes the advantage in stability. A similar line-broadening effect has been previously reported for piperidine nitroxides with bulky spiro-cyclohexyl rings in the positions 2 and 6 of the heterocycle [25, 26].

In order to clarify the nature of line broadening in the EPR spectra of the nitroxides with bulky substituents and to estimate their applicability as spin probes and spin labels for pH measurements, we performed X- and W-band EPR investigations of a series of imidazoline and imidazolidine nitroxides with methyl and ethyl substituents, and corresponding quantum chemical calculations.

2 Materials, Methods and Computational Details

2.1 Synthesis

The nitroxide radicals were synthesized according to the previously described methods (In1 [27], In2, In3, In5–In10 [28], In4, Im2 and Im1 [29], see Table 1; Scheme 1).

3,4-Dimethyl-2,2,5,5-tetraethyl-perhydroimidazole-1-oxyl-D_9+ (In4d) was synthesized according to the procedure proposed for non-deuterated nitroxide In4 using bromoethane-D_5 and D_2O as isotope-containing starting materials (Scheme 1). 3-Pentanone was repeatedly stirred with 5% solution of NaOD in D_2O until methylene proton signals disappeared in the nuclear magnetic resonance ^1H spectrum, dried with $MgSO_4$ and distilled. The 3-pentanone-D_4 (10 ml, 0.09 mol) was added dropwise to ethylmagnesium bromide solution, prepared from bromoethane-D_5 (11.4 g, 0.1 mol), Mg (3 g, 0.125 mol) and dry diethyl ether (50 ml). After addition was over, the reaction mixture was stirred for 1 h and quenched with saturated NaCl solution. The organic layer was separated, dried with Na_2CO_3 and the ether

was distilled off. Iodine (50 mg) was added to the residue and the mixture was heated to boiling, and 3-ethylpentene-2-D_7 formed was slowly distilled with water. The organic layer was separated, dried with $MgSO_4$ and distilled again. 3-Ethyl-pentene-2-D_7 was then converted into 3-hydroxyamino-3-ethylpentan-2-one-D_5 hydrochloride using the procedures described for non-deuterated compounds; overall yield was 5.9 g (32%). The obtained material (3 g, 16 mmol) was enriched with deuterium using repetitive dissolving in methanol-D and evaporation of the solvent under reduced pressure. Then ND_4OAc (4.9 g, 60 mmol), 3-pentanone-D_4 (5.4 g, 60 mmol) and methanol-D (5 ml) were added, the reaction mixture was thoroughly degassed using bubbling with argon and sealed up. The mixture was stirred for 21 days under argon, then the flask was opened and the solvents were removed under reduced pressure. The residue was dissolved in water (30 ml), basified with $NaHCO_3$ and extracted with diethyl ether. The extract was washed with water, and dried with Na_2CO_3. Then MnO_2 (4 g, 46 mmol) was added and the mixture was stirred for 1 h. The manganese oxides were filtered off, ether was removed under reduced pressure and the residue was separated using column chromatography on silica gel (eluent hexane–diethyl ether, 20:1) to give 2.1 g (57%) of 4-methyl-2,2,5,5-tetraethyl-2,5-dihydroimidazole-1-oxyl-D_9+. The latter was then converted into nitroxide In4d using the procedures described for non-deuterated compounds.

2.2 X-Band EPR Characterization of Nitroxides in Aqueous Solutions

The 0.5 mM nitroxide solutions were prepared by dissolving in water containing 0.01 M HCl or 0.01 M NaOH. The poorly soluble nitroxides were first dissolved in acetone or dimethyl sulfoxide (DMSO) and then added to the solution (the content of acetone or DMSO in final solutions was less than 5%). EPR spectra were recorded on a Bruker ER-200D-SRC or Bruker EMX spectrometer using 50 μl quartz capillaries with an inner diameter ID = 0.8 mm, placed in a rectangular TE_{102} resonator. Typical experimental EPR settings were: sweep width, 60 G; microwave power, 10 mW; modulation frequency, 100 kHz; modulation amplitude, 0.5 G; time constant, 40.96 ms; sweep time, 83.89 s; number of points, 1,024; and harmonic, first. Simulation of EPR spectra was performed using the WINSIM software [30].

2.3 X-Band EPR Characterization of Nitroxides in Toluene at Various Temperatures

Nitroxides (50 μM) In2, 3, and 4 were dissolved in toluene, deoxygenated by several freeze–pump–thaw cycles to 10^{-5} mbar, and sealed off under 100 mbar of He in conventional EPR tubes with an inner diameter of 3 mm. EPR spectra were recorded on an EMX spectrometer (Bruker) equipped with a temperature controller at various temperatures. Typical EPR settings were: sweep width, 10–15 G; microwave power, 10 mW; modulation amplitude, 0.5 G; time constant, 40.96 ms; sweep time, 83.89 s; and number of points, 1,024.

2.4 W-Band EPR Characterization of Nitroxides

The W-band EPR spectra (95 GHz/3.4 T) were recorded on laboratory-built spectrometers described elsewhere [31, 32]. Nitroxides (50 μM) were dissolved in buffer solution with addition of 30% of glycerol and placed into capillaries with an inner diameter of 0.1 mm. EPR spectra of frozen solutions were simulated using the EasySpin software [33].

2.5 Quantum Chemical Calculations

Geometries of a series of conformations of the imidazoline and imidazolidine nitroxides with different alkyl substituents at positions 2 and 5 of the heterocycle were optimized at the UB3LYP/6-31G(d) level [34, 35]. The hyperfine splitting (hfs) constants were calculated at the same level of theory. All calculations were performed with the Gaussian-03 [36] suite of programs. The influence of a solvent on the hfs constants was taken into account using the

polarizable continuum model [37]. The results of the UB3LYP calculations did not suffer from the spin contamination effects; the expectation values of S^2 were within 0.754–0.756 for all studied radicals.

3 Results and Discussion

3.1 X-Band EPR Characterization of the Substituted Imidazoline and Imidazolidine Nitroxides

The EPR spectra of the imidazoline (Im) and imidazolidine (In) nitroxides in liquid solution show a triplet pattern resulting from hfs on the ^{14}N ($I = 1$) atom of N–O· moiety. Reversible protonation of the N-3 atom of the radical heterocycle (see Scheme 1) affects spectroscopic parameters (hfs constants, *g*-factors), which allows to measure pH changes using the EPR technique [17]. The structures of imidazoline-type (Im) and imidazolidine-type (In) nitroxides studied in this paper are represented in Scheme 1.

The pK_a values of the imidazolidine nitroxides lay in the range of 4.3–5 [38], e.g., pK_a are equal to 4.7 for In1, 4.7 for In3, and 4.95 for In4 [24], whereas for imidazoline, pK_a are equal to 1.3 for Im1 and 1.2 for Im4 [24]. The parameters of protonated and deprotonated forms were determined using the procedure similar to that described in Ref. [17]. First, the pH dependence of the EPR spectra was measured, and then the observed two superimposed triplets (at pH close to pK_a) as well as hfs and *g*-factors of these triplet spectra were assigned to protonated and deprotonated forms. The measured parameters of the EPR spectra correspond to $pH \ll pK_a$ (0.01 M HCl, pH 2) and $pH \gg pK_a$ (0.01 M NaOH, pH 12) for protonated and deprotonated forms, respectively. The EPR spectra measured at these specific conditions were assigned to the protonated and deprotonated forms of the radicals.

The replacement of methyl groups by ethyl groups at positions 2 and 5 of the heterocycle results in broadening of the components of the EPR spectra of Im nitroxides and in revealing additional hfs of the EPR lines for In nitroxides. Figure 1 shows the EPR spectra of protonated tetramethyl substituted (Im1, spectrum A) and tetraethyl substituted (Im2, spectrum B) imidazoline nitroxides measured in 0.01 M HCl. The line width increased from 0.083 mT for Im1 to 0.152 mT for Im2, apparently due to additional unresolved hfs on protons of ethyl groups. A similar effect was observed for deprotonated forms of the nitroxides measured in 0.01 M NaOH (data not shown).

The EPR spectra of 0.01 M HCl solutions of 2,2,5,5-tetramethyl-4-methyl-substituted imidazolidine (In1, spectrum A), 2,2-diethyl-5,5-dimethyl-4-methyl-substituted imidazolidine (In2, spectrum B), 2,2-dimethyl-5,5-diethyl-4-methyl- substituted imidazolidine (In3, spectrum C), and 2,2,5,5-tetraethyl-substituted imidazolidine (In4, spectrum D) nitroxides are shown in Fig. 2. In contrast to imidazoline nitroxides, the introduction of two ethyl groups at position 2 or 5 of the imidazolidine heterocycle resulted in appearance of an additional doublet splitting of each ^{14}N hyperfine line of the EPR spectrum (see Fig. 2b, c). Moreover, substitution of all methyl groups by ethyl groups at both positions 2 and 5 of the heterocycle resulted in additional quadruplet splitting (see Fig. 2d; Table 1).

As mentioned above, the nitrogen hfs constant depends on the medium pH. In order to verify the pH dependence of additional splitting, the EPR spectra were measured for both the protonated and deprotonated forms of nitroxides. As an example, Fig. 3 presents the EPR spectra of protonated and deprotonated forms of imidazolidine nitroxide In3 measured in 0.01 M HCl and 0.01 M NaOH, respectively. Both the hfs constants on the ^{14}N-1 atom and additional doublet hfs were found to be significantly different in protonated and deprotonated forms and are summarized in Table 1. Note that nitrogen hfs constants

decrease upon protonation, whereas additional hfs constants assigned to protons increase (see Table 1; Fig. 3).

A similar observation of proton hyperfine splitting was published by Khramtsov et al. [1] for 5,5-dimethyl-2-methoxy-2-(2-methoxycarbonylethyl)-4-phenyl-2,5-dihydroimidazole-1-oxyl 3-oxide [4]. The authors [1] were able to measure the splitting constant of about 0.07 mT assigned to hyperfine interaction with one of the methylene protons of the $(CH)_2COOCH_3$ group. This hfs was found to be temperature-dependent, decreasing upon temperature increase. A similar dependence of the proton hfs constant on temperature was observed for diethyl- and tetraethyl-substituted imidazolidines In2, In3, and In4 as illustrated in Figs. 4 and 5. Figure 4 represents the second derivative of the central component of the EPR spectra of the In nitroxides dissolved in toluene. The proton hfs constants decreased with increasing temperature, resulting in the collapse of the doublet splitting into an unresolved singlet line at temperatures above 350 K in the case of In2. Figure 5 shows the temperature dependence of the proton hfs for ethyl-substituted imidazolidines In2, In3, and In4.

It is clear that the observed temperature dependences of the additional splitting and line broadening indicate the conformational changes in the nitroxide molecules. Note that there are four protons of two CH_2 groups at each of the positions 2 and 5 of the radical heterocycle, whereas hfs of only one proton is evident in the EPR spectra (see Figs. 2, 4). In order to interpret the EPR spectra of the nitroxides In2, In3, and In4 and their temperature dependences, we employed the quantum chemical calculations.

Magnetic properties of a series of nitroxides, including 2,2,5,5-tetramethyl-4-methyl-imidazoline nitroxide, Im1, have been previously analyzed in detail using density functional theory (DFT) calculations [39, 40]. It is well documented that all DFT methods underestimate the absolute values of isotropic hfs constants of the nitrogen atom of nitroxides (a_N). These hfs constants could be quantitatively predicted using high-level calculations as well as vibrational averaging. Moreover, the formation of nitroxide complexes with two water molecules should be taken into account to predict quantitatively the a_N value in water. Taking all these effects into account provide the possibility to calculate the magnetic titration curve for Im1 in quantitative agreement with the experiment [40].

On the other hand, it is well known that simple B3LYP calculations predict fairly well the hfs constants of hydrogen atoms of organic radicals [39, 41]. The main purpose of our calculations is to reveal the influence of the alkyl substituents at positions 2 and 5 on the EPR spectra of nitroxides. Therefore, we employed the simple B3LYP/6-31G(d) method to calculate the hfs constants and free energies of different conformations of In and Im nitroxides, and the free energy of activation for the transitions between these conformers.

Figure 6 represents calculated hfs constants of nitrogen and hydrogen atoms of nitroxide In1 and In4. The hfs constants of methyl groups are usually averaged due to their fast rotation around the C–C bond on the EPR time scale. The averaged values are very low (0.01 mT) and contribute only to small broadening of the EPR lines. The calculations predict that the free energy of activation for the rotation of methyl groups at position 5 (In1) is 4.4 kcal/mol. The rate constant of this rotation at room temperature is calculated to be 3.9×10^{-9} s^{-1}, which is really fast on the EPR time scale.

Figure 6b displays the hfs constants calculated for one of the low-energy conformers of tetraethyl-substituted imidazolidine, In4. It demonstrates that only two a_H values for four CH_2 groups are high enough (about 0.23 mT), the absolute values of all others do not exceed 0.05 mT. Similar situation was observed for all conformers optimized for rotation of ethyl

groups. The a_H constants for methyl groups were averaged as the rate constant of their rotation at room temperature is calculated to be 2.2×10^{10} s^{-1}.

To interpret the temperature dependence of the experimental a_H values we analyzed the dynamics of the radical structure. As a matter of fact, two types of motions can modulate a_H hfs constants, notably, the rotation of alkyl groups and the ring puckering. We calculated stationary points on the potential energy surface (PES) for the ring puckering of unsubstituted nitroxide In1 and its derivatives, In2 and In4. Figure 7 demonstrates that conformers of unsubstituted nitroxide In1 have the same energy and ring puckering proceeds at room temperature with a high rate constant ($k \sim 10^{10}$ s^{-1}). Situation is different in the case of nitroxides In2 and In4, notably, one conformer is much more preferable than the other. Thus, calculations predict that ring puckering does not lead to noticeable averaging of the a_H hfs constants of nitroxides In1 and In4.

In addition, we calculated the stationary points on the PES for rotation of ethyl groups. There is a large set of minima on the PES for rotation of ethyl groups in the tetraethyl-substituted In4. The free energies of different structures obtained by rotation of ethyl groups at position 2 were predicted to differ within 3 kcal/mol. The free energies of activation for these rotations were predicted within 6.5–7.7 kcal/mol. Thus, these rotations have enough low rate constants at room temperature (in the range of 10^7–10^8 s^{-1}). Therefore, calculations predict that additional splitting of about 0.2 mT in the EPR spectra of ethyl-substituted imidazolidines arises from the hfs constant of only one of four methylene hydrogens of two geminal ethyl substituents. The rotation of the ethyl groups is retarded when compared to methyl groups due to sterical hindrance, and the hfs constants of the protons of methylene groups are not rotationally averaged in contrast to those of methyl groups.

To confirm the assignment of the a_H constants, the deuterium-substituted imidazolidine In4d (see Scheme 1; Table 1) was synthesized. Figure 8 presents the EPR spectra of In4 and In4d nitroxides in water solution at pH 3.0 at X-band (spectrum A) and W-band (spectrum B). The most important difference between these spectra is the presence of splitting in the spectrum of In4 radical and its absence in the spectrum of its deuterated analog In4d. These data unambiguously confirm that additional hfs constants originate from methylene protons of the ethyl groups.

Temperature dependences of the observed a_H constants shown in Figs. 4 and 5 could be used to estimate the activation energy of transitions between the conformers. Unfortunately we failed to simulate the EPR spectra of In2, In3 and In4 at different temperatures by taking into account the exchange interaction and assuming different contributions of the Gaussian and Lorentzian shapes. The estimated rate of exchange (assuming the two-position model), with taking into account the a_H values of 0.25 mT at $T = 175$ K and 0.16 mT at 365 K, is in the range of 5×10^6–2.5×10^7 s^{-1} for $T = 200$–350 K. The obtained values of activation energy lie in the range of 2–1.5 kcal/mol for In2 and 1.5–0.7 kcal/mol for In3, and the pre-exponential factors are in the range of 10^7–10^8 s^{-1}. The obtained values of activation energy and pre-exponential factors are unreasonably low. The reason for this can be the use of a simplified two-position model for a complicated process of transition between a big set of conformers with different relative energies.

As discussed above, the calculations predict relatively high activation energy for ethyl group rotation, implying that the observed spectra of In2, In3, and In4 at ambient temperatures should correspond to slow-to-medium exchange on the EPR time scale. Meanwhile, calculations predict for all low-energy conformers only one large a_H constant (ca. 0.2 mT) for a pair of geminal ethyl groups. The superposition of spectra of different conformers with similar hyperfine structures could not be excluded. Temperature elevation leads to increase

of the rate of transitions between the conformers with partial or complete averaging of a_H, leading to decrease or disappearance of splitting. The hfs averaging is more effective for 2,2-diethyl-substituted nitroxide In2 than for 5,5-diethyl-substituted In3 (Figs. 6, 7), presumably due to the contribution of the ring puckering into averaging.

The EPR spectra of other sterically substituted nitroxides, In5–In10 (see Scheme 1; Table 1), were studied revealing additional hfs on hydrogens similar to that for In1–In4 (see Table 1). The difference between In6 and In7 (resolved additional hfs on hydrogen for In7 and the absence of additional hfs for In6) is determined by the conformationally more rigid structure of the cyclohexyl ring in In7 in comparison with the cyclopentyl ring in In6.

It is worth to note that we were unable to resolve splitting in the EPR spectrum of tetraethyl-substituted nitroxide Im2. The difference in hyperfine structure of the spectra of Im and In nitroxides results from the difference in geometry of the rings. Due to the planar geometry of the imidazoline ring the rotation of ethyl groups in these nitroxides is less hindered and leads to more effective hfs averaging.

3.2 W-Band EPR Characterization of the Substituted Imidazoline and Imidazolidine Nitroxides

It was demonstrated previously that W-band EPR spectroscopy allows the pK_a determination from the precise *g*-factor measurements. To check the pH-sensitivity of the nitroxides with bulky substituents we employed W-band spectroscopy for the measurement of *g*-factor changes in frozen solutions. Figure 9 shows the W-band EPR spectra of In4 and its deuterium-substituted analogue In4d in protonated and deprotonated forms measured at 180 K. The low-temperature W-band spectra are typical for the frozen-solution continuous-wave EPR spectra of the nitroxide radicals. They were simulated using a powder pattern and assuming anisotropic hyperfine interaction with the spin of ^{14}N nucleus ($I = 1$) and an anisotropic **g**-tensor. Both tensors were supposed to be diagonal in the molecular frame of the nitroxides.

Dashed lines in Fig. 9 represent the best fits to the experimental EPR spectra obtained using the EasySpin software [33]. The parameters of simulations (the canonical values of the ^{14}N hfs and **g**-tensors) are listed in Table 2 together with the values predicted at the UB3LYP/6-31G(d) level. The individual line shape was assumed to be Gaussian with a line width of 0.7 mT. For In4, the a_H constants obtained by X-band EPR at room temperatures (Table 1) were taken into account. It is seen from Fig. 9 that protonation leads to the substantial change in the g_{xx} component and does not affect the g_{zz} value. The increase of the g_{xx} value upon protonation of In4 by 6.4×10^{-4} is very close to the same value reported for In1 (6.5×10^{-4}) [43]. Thus, the substitution by bulky substituents does not change the pH-sensitivity of *g*-factors of nitroxides while substantially increases their stability.

4 Conclusions

The X- and W-band EPR and quantum chemical studies of the magnetic resonance properties of a series of imidazolidine nitroxides with different alkyl substituents at positions 2 and 5 of the heterocycle demonstrated that an additional splitting of about 0.2 mT in the EPR spectra of ethyl-substituted imidazolidines arises from the hfs constant of only one of four methylene hydrogen atoms of two geminal ethyl substituents. The substantial narrowing of EPR lines in the spectrum of 2,2,5,5-tetraethyl-substituted imidazolidine nitroxide could be achieved by substitution of hydrogen atoms in CH_2 groups with deuterium. This finding could be used in the design of spin probes for biochemical applications.

The observed phenomenon is likely to be of general nature. Slow conformation changes in nitroxides with bulky substituents at α-carbons may lead to the line broadening of their EPR spectra. Moreover, this problem can hardly be completely overcome by isotope substitution. Thus, rigid structures seem to be preferable in molecular design of spin probes.

Nevertheless, the imidazolidine radicals with bulky substituents are very perspective pH-probes for in vivo application due to their low reduction rates in living tissues. Deuteration of ethyl groups substantially decreases the EPR line width without changes in the reduction rates. This could be useful for many biochemical and biomedical applications, e.g., pH-monitoring in the stomach [44]. W-band EPR study of 2,2,5,5-tetraethyl-substituted imidazolidine nitroxide and its deuterium-substituted analog at low temperatures of their *g*-factors to pH, which indicates their applicability as site-directed labeling probes possessing high stability.

Acknowledgments

Support by the Russian Foundation for Basic Research (grants 08-04-00555 and 08-04-00432), Russian Federal Ministry of Science and Education (P 1144), Siberian Supercomputer Center is gratefully acknowledged. A.B. and V.K. acknowledge the support of National Institutes of Health (grants HL089036 and CA132068). We are thankful to Dr. Anton Savitsky (Free University of Berlin) for the measurements of W-band spectra.

References

1. Swartz HM, Clarkson RB. Phys. Med. Biol. 1998; 43:1957–1975. [PubMed: 9703059]
2. Velan SS, Spencer RG, Zweier JL, Kuppusamy P. Magn. Reson. Med. 2000; 43:804–809. [PubMed: 10861874]
3. Foster MA, Grigor'ev IA, Lurie DJ, Khramtsov VV, McCallum S, Panagiotelis I, Hutchison JM, Koptioug A, Nicholson I. Magn. Reson. Med. 2003; 49:558–567. [PubMed: 12594760]
4. Khramtsov VV, Weiner LM, Gogolev A, Grigor'ev IA, Starichenko VF, Volodarsky LB. Magn. Reson. Chem. 1986; 24:199–207.
5. Khramtsov VV, Grigor'ev IA, Foster MA, Lurie DJ. Antioxid. Redox Signal. 2004; 6(3):667–676. [PubMed: 15130294]
6. Roshchupkina GI, Bobko AA, Bratasz A, Reznikov VA, Kuppusamy P, Khramtsov VV. Free Radic. Biol. Med. 2008; 45:312–320. [PubMed: 18468522]
7. Swartz HM, Khan N, Khramtsov VV. Antioxid. Redox Signal. 2007; 9:1757–1771. [PubMed: 17678441]
8. Kuppusamy P, Li H, Ilangovan G, Cardounel AJ, Zweier JL, Yamada K, Krishna MC, Mitchell JB. Cancer Res. 2002; 62:307–312. [PubMed: 11782393]
9. Yamada K, Inoue D, Matsumoto S, Utsumi H. Antioxid. Redox Signal. 2004; 6:605–611. [PubMed: 15130287]
10. Hubbel WL, Cafiso D, Altenbach C. Nat. Struct. Biol. 2000; 7:735–739. [PubMed: 10966640]
11. Winalski CS, Shortkroff S, Mulkern RV, Schneider E, Rosen GM. Magn. Reson. Med. 2002; 48:965–972. [PubMed: 12465105]
12. Keana JF, Van Nice FL. Physiol. Chem. Phys. Med. NMR. 1984; 16:477–480. [PubMed: 6537509]
13. Smirnov AI, Ruuge A, Reznikov VA, Voinov MA, Grigoriev IA. J. Am. Chem. Soc. 2004; 126:8872–8880. [PubMed: 15264799]
14. Voinov MA, Ruuge A, Reznikov VA, Grigor'ev IA, Smirnov AI. Biochemistry. 2008; 47:5626–5637. [PubMed: 18426227]
15. Tikhonov AN, Agafonov RV, Grigor'ev IA, Kirilyuk IA, Ptushenko VV, Trubitsin BV. Biochim. Biophys. Acta. 2008; 1777:285–294. [PubMed: 18226594]
16. Moebius K, Savitsky A, Wegener C, Plato M, Fuchs M, Schnegg A, Dubinskii AA, Grishin YA, Grigor'ev IA, Kuhn MK, Duche D, Zimmermann H, Steinhoff H-J. Magn. Reson. Chem. 2005; 43:4–19.
17. Khramtsov VV, Weiner LM, Grigoriev IA, Volodarsky LB. Chem. Phys. Lett. 1982; 91:69–72.

18. Kocherginsky, N.; Swartz, HM. Nitroxide Spin Labels Reactions in Biology and Chemistry. Boca Raton: CRC Press; 1995.
19. Mehlhorn RJ. J. Biol. Chem. 1991; 266:2724–2731. [PubMed: 1993652]
20. Yelinova VI, Krainev AG, Savelov A, Grigor'ev IA. J. Chem. Soc. Perkin Trans. 1993; 2(11): 2053–2055.
21. Bobko AA, Kirilyuk IA, Grigor'ev IA, Zweier JL, Khramtsov VV. Free Radic. Biol. Med. 2007; 42(3):404–412. [PubMed: 17210453]
22. Keana JFW, Pou S, Rosen GM. Magn. Res. Med. 1987; 5:525–536.
23. Marx L, Chiarelli R, Guiberteau T, Rassat A. J. Chem. Soc. Perkin Trans. 2000; 1:1181–1182.
24. Kirilyuk IA, Bobko AA, Grigor'ev IA, Khramtsov VV. Org. Biomol. Chem. 2004; 2(7):1025–1030. [PubMed: 15034626]
25. Okazaki S, Mannan MDM, Sawai K, Masunizu T, Miura Y, Takeshita K. Free Radic. Res. 2007; 41:1069–1077. [PubMed: 17886028]
26. Kinoshita Y, Yamada K-I, Yamasaki T, Sadasue H, Sakai K, Utsumi H. Free Radic. Res. 2009; 43:565–571. [PubMed: 19384748]
27. Volodarskii LB, Reznikov VA, Kobrin VS. J. Org. Chem. USSR (Engl. Transl.). 1979; 15:364–370.
28. Zubenko D, Tsentalovich Yu, Lebedeva N, Kirilyuk I, Roshchupkina G, Zhurko I, Reznikov V, Marque SRA, Bagryanskaya E. J. Org. Chem. 2006; 71:6044–6052. [PubMed: 16872187]
29. Sevastjanova TK, Volodarsky LB. Bull. Acad. Sci. USSR Div. Chem. Sci. (Engl. Transl.). 1972; 21:2276–2280.
30. Duling DR. J. Magn. Reson. B. 1994; 104:105–110. [PubMed: 8049862]
31. Fuchs MR, Prisner TF, Möbius K. Rev. Sci. Instrum. 1999; 70:3681–3683.
32. Schnegg A, Kirilina E, Fuchs M, Savitsky A, Grishin Y, Dubinskii A, Plato M, Lubitz W, Möbius K. Appl. Magn. Reson. 2007; 31:59–98.
33. Stoll S, Schweiger A. J. Magn. Reson. 2006; 178:42–55. [PubMed: 16188474]
34. Becke AD. J. Chem. Phys. 1993; 98:5648–5654.
35. Lee C, Yang W, Parr RG. Phys. Rev. B. 1988; 37:785–790.
36. Frisch, MJ.; Trucks, GW.; Schlegel, HB.; Scuseria, GE.; Robb, MA.; Cheeseman, JR.; Montgomery, JA., Jr; Vreven, T.; Kudin, KN.; Burant, JC.; Millam, JM.; Iyengar, SS.; Tomasi, J.; Barone, V.; Mennucci, B.; Cossi, M.; Scalmani, G.; Rega, N.; Petersson, GA.; Nakatsuji, H.; Hada, M.; Ehara, M.; Toyota, K.; Fukuda, R.; Hasegawa, J.; Ishida, M.; Nakajima, T.; Honda, Y.; Kitao, O.; Nakai, H.; Klene, M.; Li, X.; Knox, JE.; Hratchian, HP.; Cross, JB.; Adamo, C.; Jaramillo, J.; Gomperts, R.; Stratmann, RE.; Yazyev, O.; Austin, AJ.; Cammi, R.; Pomelli, C.; Ochterski, JW.; Ayala, PY.; Morokuma, K.; Voth, GA.; Salvador, P.; Dannenberg, JJ.; Zakrzewski, VG.; Dapprich, S.; Daniels, AD.; Strain, MC.; Farkas, O.; Malick, DK.; Rabuck, AD.; Raghavachari, K.; Foresman, JB.; Ortiz, JV.; Cui, Q.; Baboul, AG.; Clifford, S.; Cioslowski, J.; Stefanov, BB.; Liu, G.; Liashenko, A.; Piskorz, P.; Komaromi, I.; Martin, RL.; Fox, DJ.; Keith, T.; Al-Laham, MA.; Peng, CY.; Nanayakkara, A.; Challacombe, M.; Gill, PMW.; Johnson, B.; Chen, W.; Wong, MW.; Gonzalez, C.; Pople, JA. Gaussian 03 (Revision B.01). Pittsburg PA: Gaussian Inc; 2003.
37. Tomasi J, Mennucci B, Cammi R. Chem. Rev. 2005; 105:2999–3002. [PubMed: 16092826]
38. Khramtsov, VV.; Volodarsky, LB. Spin Labeling: The Next Millenium, Biological Magnetic Resonance. Berliner, LJ., editor. Vol. vol. 14. New York: Plenum Press; 1998.
39. Importa R, Barone V. Chem. Rev. 2004; 104:1231–1253. [PubMed: 15008622]
40. Importa R, Scalmani G, Barone V. Chem. Phys. Lett. 2001; 336:349–356.
41. Importa, R.; Barone, V.; Bally, T.; Borden, WT. Reviews in Computational Chemistry. Lipkowitz, KB.; Boyd, DB., editors. Vol. vol. 13. New York: Wiley; 1999. p. 1-97.
42. Savitsky A, Dubinskii AA, Plato M, Grishin YA, Zimmermann H, Möbius K. J. Phys. Chem. B. 2008; 112:9079–9090. [PubMed: 18593147]
43. Gullá AF, Budil DE. J. Phys. Chem. B. 2001; 105:8056–8062.
44. Potapenko DI, Foster MA, Lurie DJ, Kirilyuk IA, Hutchison JM, Grigor'ev IA, Bagryanskaya EG, Khramtsov VV. J. Magn. Reson. 2006; 182:1–11. [PubMed: 16798033]

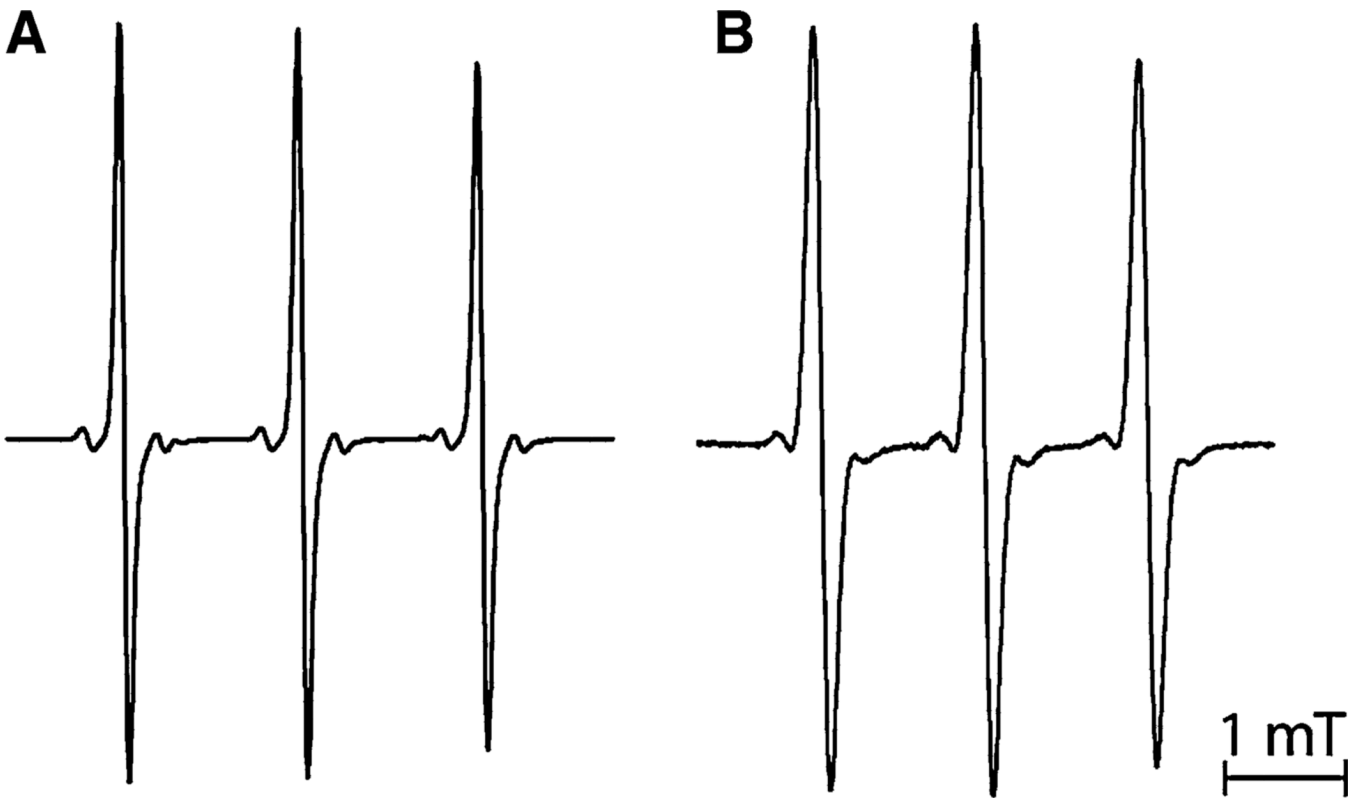

Fig. 1.
EPR spectra of 0.5 mM aqueous solutions of the imidazoline nitroxides Im1 (**a**) and Im2 (**b**) recorded in the presence of 0.01 M HCl at room temperature

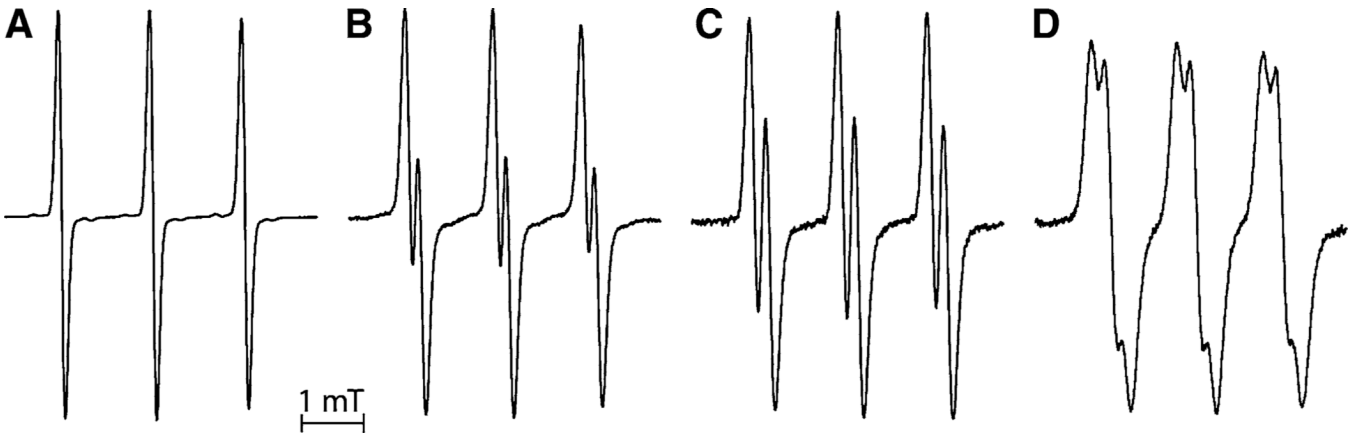

Fig. 2.

X-band EPR spectra of 0.5 mM aqueous solutions of the imidazolidine-type nitroxides In1 (**a**), In2 (**b**), In3 (**c**), and In4 (**d**) recorded in the presence of 0.01 M HCl at room temperature

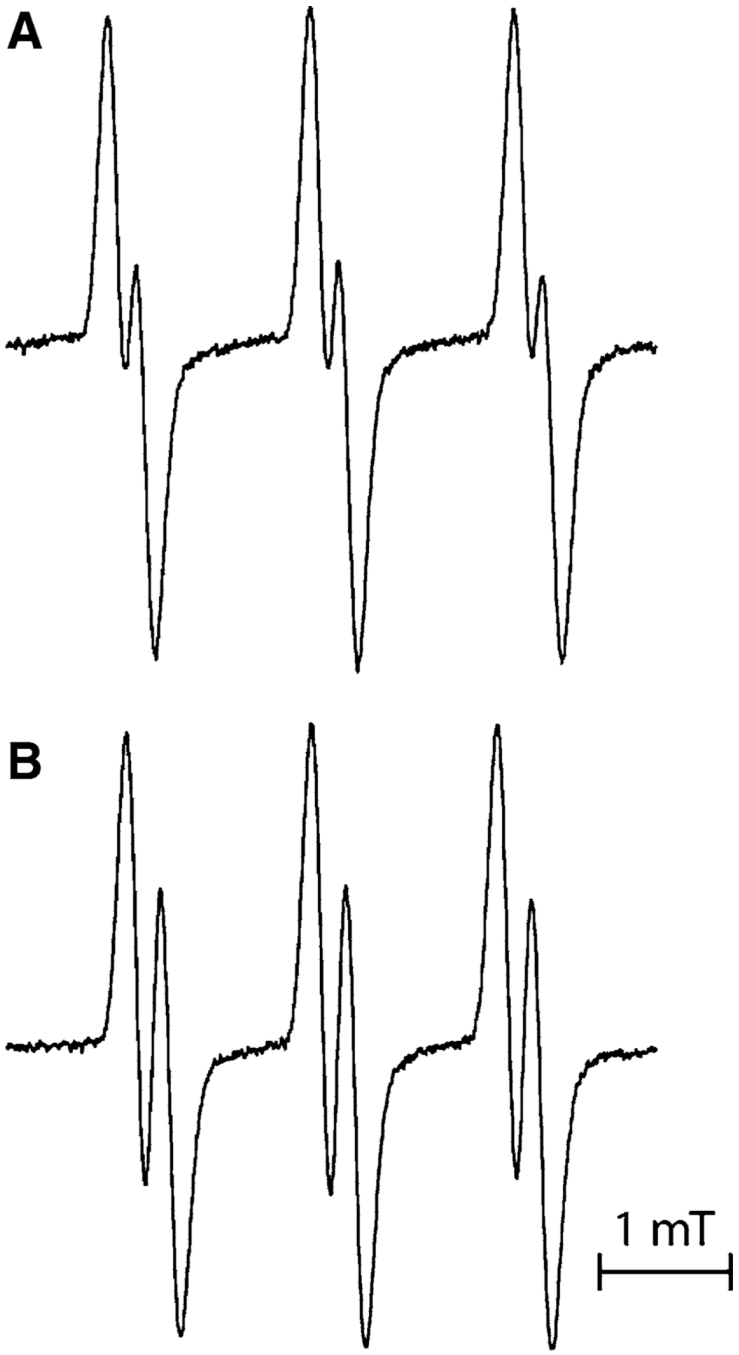

Fig. 3.
X-band EPR spectra of 0.5 mM aqueous solutions of the nitroxide In3 measured in the presence of 0.01 M NaOH (**a**) and 0.01 M HCl (**b**)

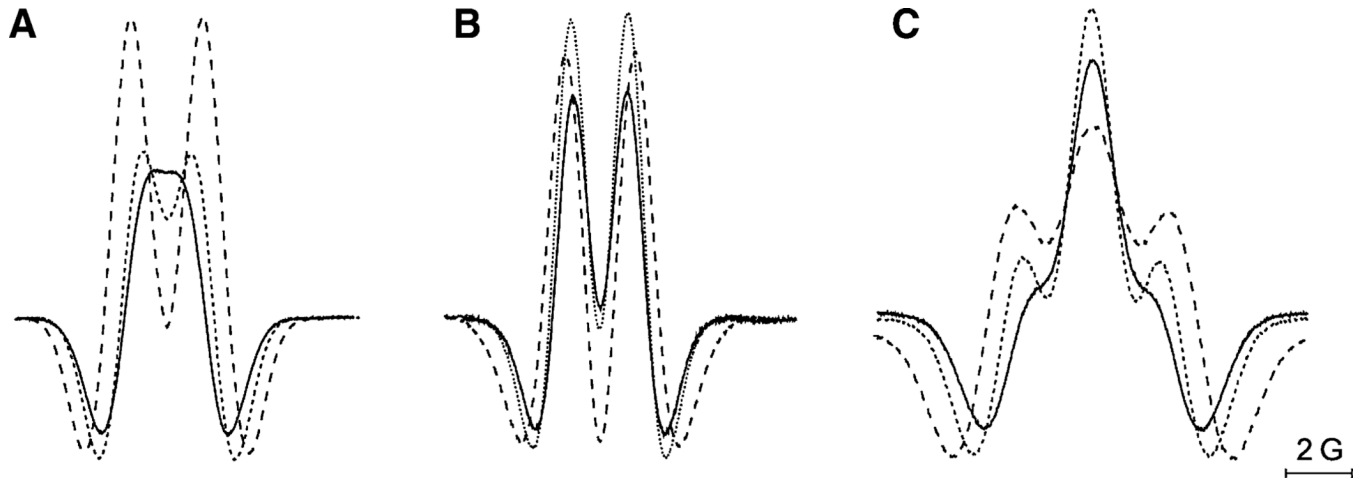

Fig. 4.

Central components of the second-derivative continuous-wave EPR spectra of imidazolidine nitroxides In2 (**a**), In3 (**b**) and In4 (**c**) measured at 250 K, *dashed line*; 300 K, *dotted line*; and 350 K (325 K for In3), *straight line*

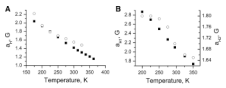

Fig. 5.

Temperature dependencies of the proton hfs constants for nitroxide In2 (*filled squares*) and In3 (*open circles*) (**a**), and In4 (**b**). Data for nitroxide In3 at temperatures above 325 K is unavailable due to radical decomposition. For nitroxide In4, two different proton hfs constants, a_{H1} and a_{H2} (see Table 1), are denoted by *filled squares* and *open circles*, respectively

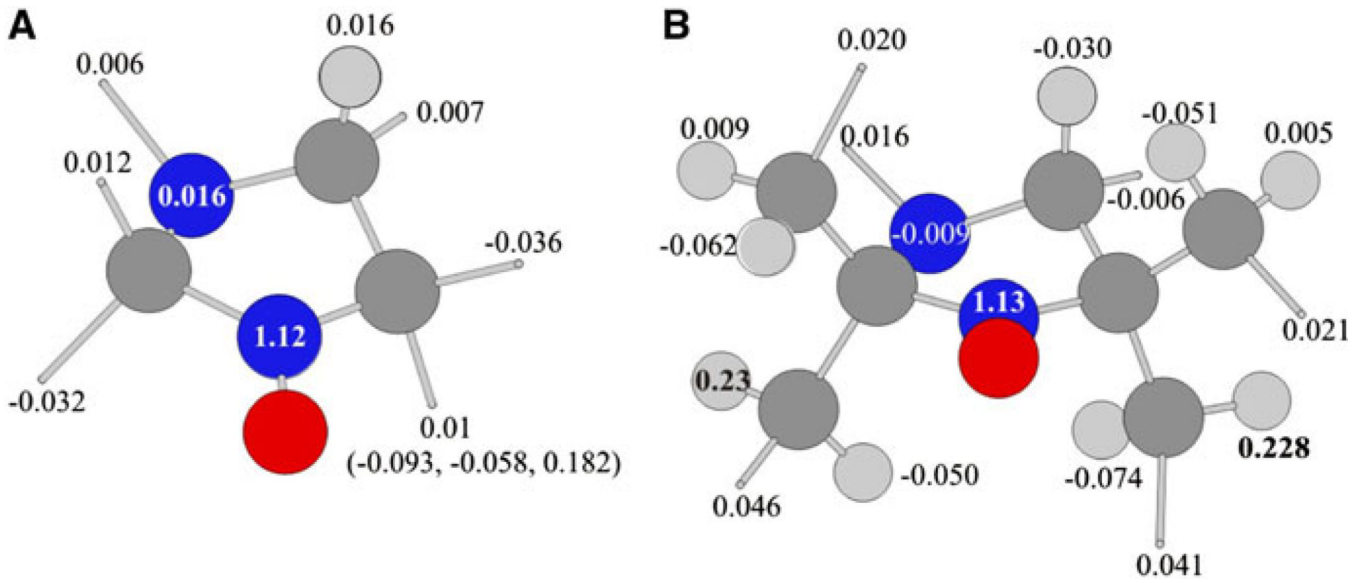

Fig. 6.

Structures of imidazolidine radicals In1 (**a**) and In4 (**b**), and values of the hfs constants calculated by the B3LYP/6-31G(d) method. For methyl groups the average values are shown. Methyl groups are represented by *gray sticks*

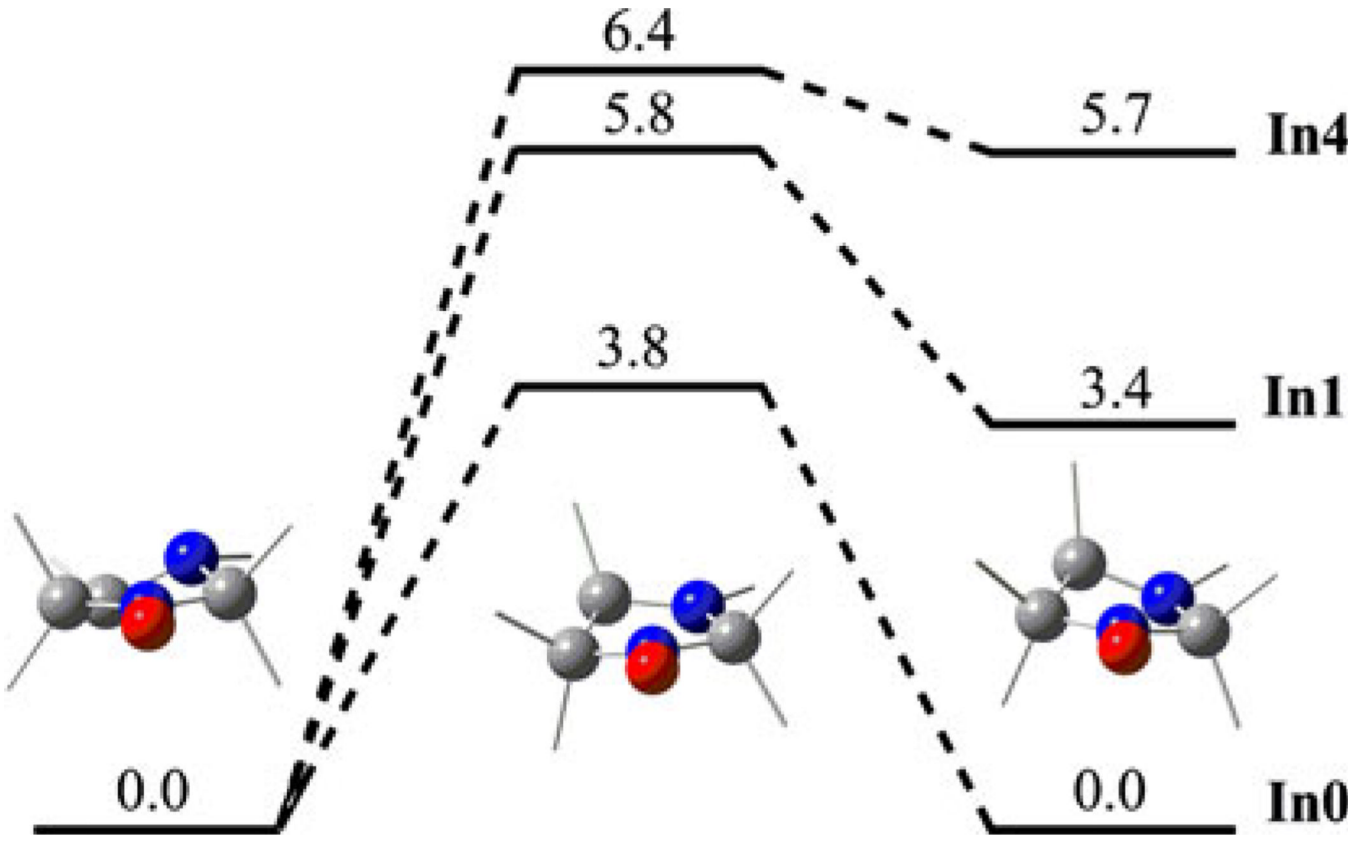

Fig. 7.
Relative free energies (in kcal/mol) of stationary points on the PES for ring puckering of the selected In nitroxides. Me and Et groups are represented by *gray sticks*

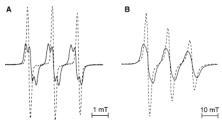

Fig. 8.

X- (**a**) and W-band (**b**) EPR spectra of 0.5 mM aqueous solutions of nitroxide In4 (*solid line*) and its deuterated analog In4d (*dashed line*) measured at pH 3.0 and temperature 293 K

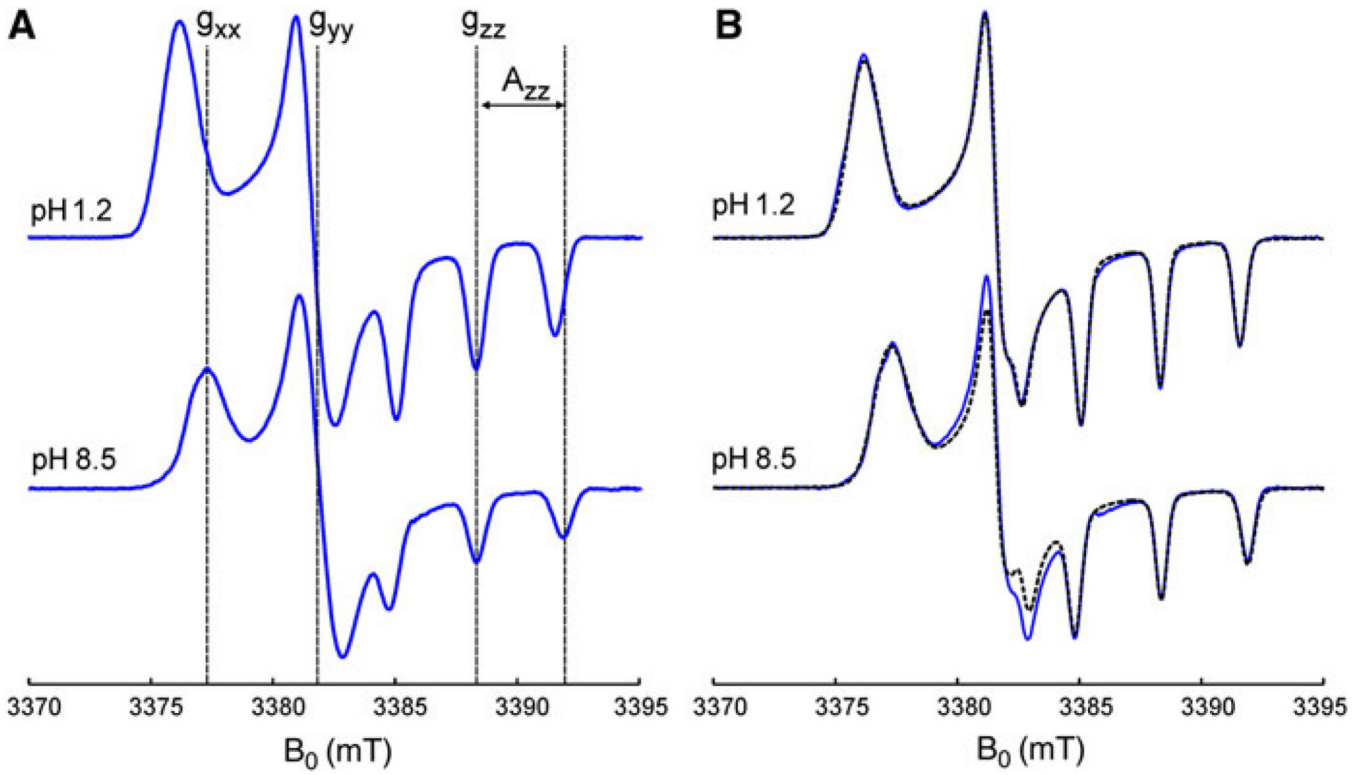

Fig. 9.

W-band continuous-wave EPR spectra of 0.5 mM tetraethyl-substituted In radicals In4 (**a**) and In4d (**b**) measured at 180 K in the mixture of glycerol (20%) and phosphate-buffered water solutions, corresponding to fully protonated (pH 1.2) and deprotonated (pH 8.5) forms of the nitroxides. The simulated spectra of In4d with magnetic parameters listed in Table 2 are shown by *dashed lines*

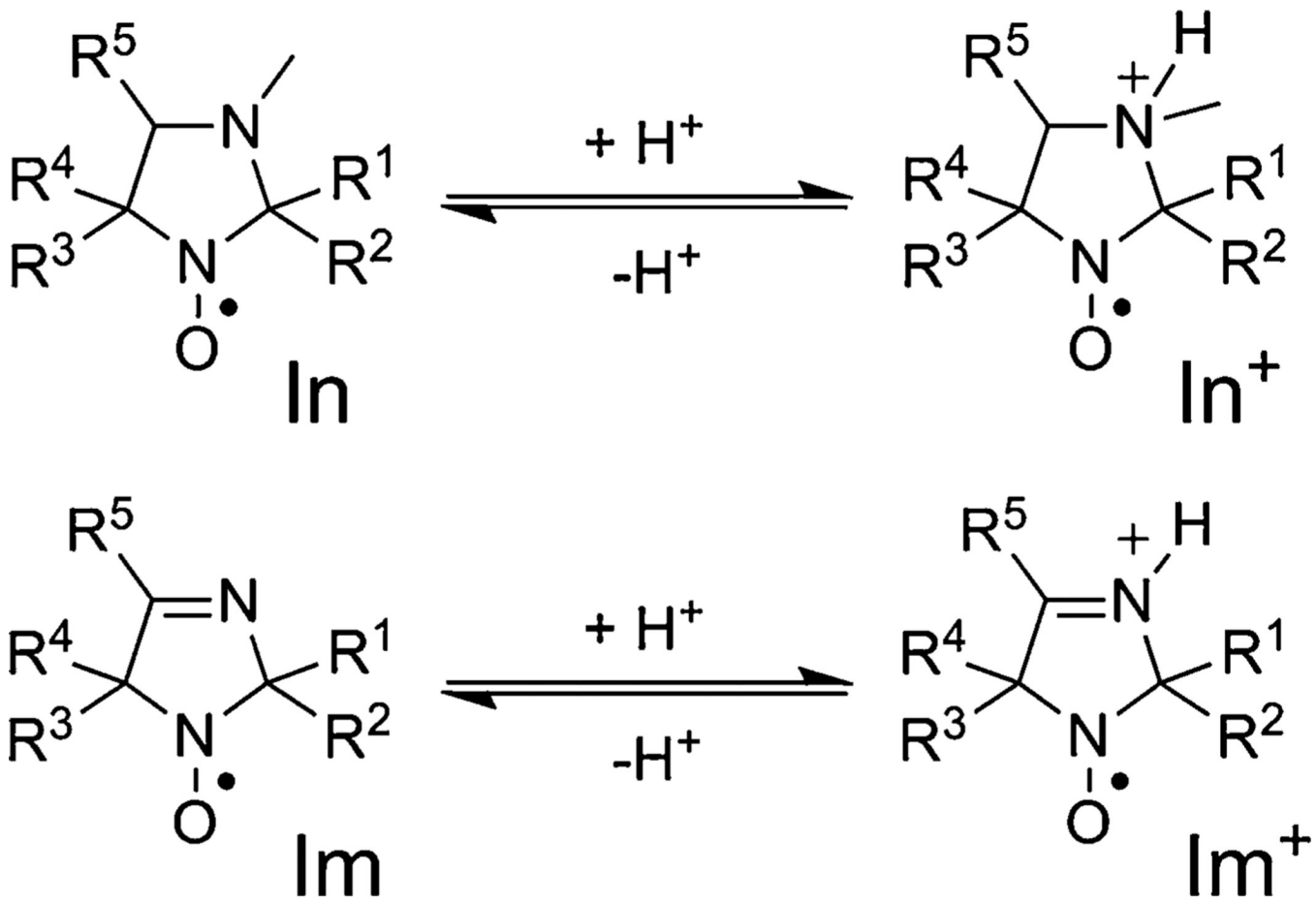

Scheme 1.
Reversible protonation of imidazoline (Im) and imidazolidine (In) nitroxides. For R^i see Table 1

Table 1

Spectroscopic parameters of the imidazoline (Im) and imidazolidine (In) nitroxides and their protonated forms (in parenthesis)

	R_1	R_2	R_3	R_4	R_5	a_N (mT) H_2O/NaOH (H_2O/HCl)	a_{H1} (mT) H_2O/NaOH (H_2O/HCl)	a_{H2} (mT) H_2O/NaOH (H_2O/HCl)	a_N (mT) toluene	a_{H1} (mT) toluene	a_{H2} (mT) toluene
Im1	Me	Me	Me	Me	Me	1.566 (1.480)	−/−	−/−	1.422	–	–
Im2	Et	Et	Et	Et	Me	1.517 (1.418)	−/−	−/−	1.374	–	–
In1	Me	Me	Me	Me	Me	1.601 (1.476)	−/−	−/−	1.439	–	–
In2	Et	Et	Me	Me	Me	1.552 (1.420)	0.143 (0.191)	−/−	1.385	0.143	–
In3	Me	Me	Et	Et	Me	1.569 (1.432)	0.201 (0.245)	−/−	1.398	0.158	–
In4	Et	Et	Et	Et	Me	1.528 (1.392)	0.242 (0.256)	0.181 (0.205)	1.369	0.206	0.173
In4d	CD_2CH_3	CD_2CH_3	CD_2CH_3	CD_2CH_3	Me	1.530 (1.395)	−/−	−/−			
In5	C_4H_9	C_4H_9	Me	Me	Me	1.566 (1.436)	0.140 (0.190)	−/−			
In6	$(CH_2)_4$		Me	Me	Me	1.614 (1.476)	−/−	−/−			
In7	$(CH_2)_5$		Me	Me	Me	1.593 (1.465)	0.274 (0.275)	−/−			
In8	$(CH_2)_5$		Et	Et	Me	1.544 (1.408)	0.250 (0.270)	0.070 (0.090)			
In9	Me	Me	Me	$(CH_2)_4$		1.614 (1.484)	0.137 (0.124)	−/−			
In10	$(CH_2)_5$		Me	$(CH_2)_4$		1.620 (1.495)	0.270 (0.272)	0.063 (0.063)			

Accuracy of hyperfine splitting constants measurement is 0.007 mT

Table 2

Magnetic parameters of tetraethyl-substituted In radicals obtained from the analysis of the W-band EPR spectra and the results of DFT calculations

Radical	g_{xx}	g_{yy}	g_{zz}	A_{xx} (mT)	A_{yy} (mT)	A_{zz} (mT)
In4d (pH 8.5)	2.00860	2.00577	2.00214	0.45[a]	0.48[a]	3.51
Calculated	2.00952	2.00590	2.00206	0.67	0.69	3.23
In4d (pH 1.2)	2.00928	2.00590	2.00215	0.38[a]	0.42[a]	3.26
Calculated	2.01001	2.00592	2.00206	0.60	0.68	2.87

[a] A_{xx} and A_{yy} values are evaluated from experimental W-band three-pulse electron spin echo envelope modulation spectra (data not shown) as described previously [42]